Engineering Structures 178 (2019) 309–317

Contents lists available at ScienceDirect

Engineering Structures

journal homepage: www.elsevier.com/locate/engstruct

A simple corrosion fatigue design method for bridges considering the coupled corrosion-overloading effect

Lu Deng, Wangchen Yan*, Lei Nie

Key Laboratory for Damage Diagnosis of Engineering Structures of Hunan Province, Hunan University, Changsha 410082, China

ARTICLE INFO

Keywords:
Coupled effect
Corrosion
Overloading
Fatigue design
Steel girder bridge

ABSTRACT

Corrosion fatigue is more detrimental than either corrosion or overloading applied separately. Nevertheless, corrosion was not explicitly covered in the AASHTO LRFD fatigue design specifications, which may lead to underestimation of the fatigue damage of bridges. Moreover, simple approaches to evaluating the fatigue life of corroded steel components are still lacking. In this study, a steel girder bridge was adopted to study the coupled corrosion-overloading effect on the fatigue life of bridges. The variation of stress range, equivalent number of stress cycle, and the resulted cumulative fatigue damage under different corrosion and overloading conditions were investigated. Then, a simple corrosion fatigue design method was proposed by considering the coupled corrosion-overloading effect which covers the individual effects due to pure overloading, pure corrosion, and the corrosion-overloading interaction. The results showed that the relationship between the corrosion-overloading interaction and the corrosion depth can be well described by an exponential function which is applicable for different overloading and corrosion conditions. Moreover, the coupled corrosion-overloading effect can greatly reduce the fatigue life of bridges and should be carefully considered in bridge fatigue design wherever necessary.

1. Introduction

Corrosion fatigue, which is referred to the joint interaction of corrosive environment and repeated vehicle loading, is more detrimental than that of either one applied individually to bridge structures [1–3]. Corrosion damage is responsible for the structural deficiency of approximately 15% of bridges in the United States [4]. However, corrosion damage was not explicitly covered in the AASHTO LRFD fatigue design specifications which were based on fatigue tests data obtained in clean and dry air conditions in the laboratory [5–9]. Therefore, the AASHTO fatigue design may underestimate the fatigue damage of bridges under corrosive environment.

Much research has been devoted to studying the corrosion fatigue damage on bridges. From 1920s, McAdam [10] started a comprehensive fatigue test program for carbon and low alloy steels in corrosive environment and found that their corrosion fatigue strengths were relatively low. In 1980s, Kayser and Nowak [11] conducted field surveys to investigate various types of corrosion on bridges and attempted to determine the influence of corrosion on bridge safety based on reliability analysis. Recently, Cha et al. [12] conducted a numerical analysis of the effect of overloading and corrosion on the fatigue life of steel bridges based on the finite element model updating technique. In their analysis, the total fatigue damage was considered as a sum of the damage caused by repetitive truck loading and the damage due to the corrosive environment. In other words, the effects of corrosion and overloading were considered as two separate processes rather than a coupling process. In fact, the bridge stress is closely related to the corrosion condition due to their interaction, i.e., the stress increases with the growth of corrosion rate, and vice versa [1].

To further investigate the coupled corrosion-fatigue damage, Yang et al. [3] conducted a theoretical study to analyze the deterioration mechanism of bridge deck slabs and demonstrated that the coupled corrosion fatigue effect could apparently reduce the fatigue life of bridge deck slabs. Moreover, Yang et al. [1] performed an electrochemical experiment to assess the coupled corrosion fatigue damage of welded ship structure and explored the relationship between the load and corrosion rate of steels. Zhang and Yuan [2] adopted a reliability-based approach to investigate the coupled corrosion fatigue effect on the safety of steel bridges and found that coupling effect could even cause a destructive failure. However, simple approaches to evaluating the fatigue life of corroded steel members are still lacking [13].

In the present study, a composite steel girder bridge was adopted to investigate the coupled corrosion-overloading effect on the fatigue life of bridges. The corrosion-overloading coupling process was realized by adopting the deteriorated cross section of the steel girder due to corrosion when calculating the bridge responses under the action of truck

* Corresponding author.
E-mail addresses: denglu@hnu.edu.cn (L. Deng), ywchener@berkeley.edu (W. Yan), nielei@hnu.edu.cn (L. Nie).

https://doi.org/10.1016/j.engstruct.2018.10.028
Received 5 April 2018; Received in revised form 10 August 2018; Accepted 12 October 2018

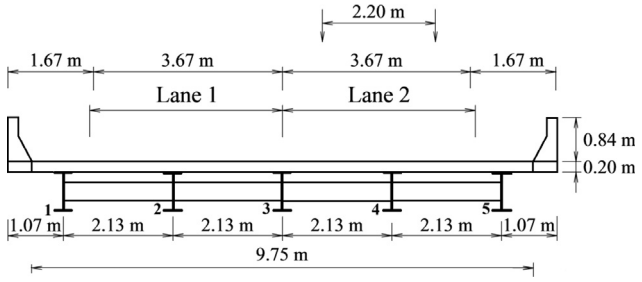

Fig. 1. Cross section of the bridge under consideration.

overloading. The variations of stress range, equivalent number of stress cycle, and the cumulative fatigue damage under different corrosion and overloading conditions were then investigated. Finally, a simple corrosion fatigue design method considering the coupled corrosion-overloading effect was proposed.

2. Numerical models

2.1. Steel girder bridge model

In this study, a typical composite bridge with steel I-girders was chosen in the numerical study. The bridge was designed according to the American Association of State Highway and Transportation Officials (AASHTO) *Standard specifications for highway bridges* [14]. This bridge model is a good representative of the simply-supported multi-girder steel-concrete composite bridges in the United States, and has been widely used to study the performance of bridges [15,16]. The bridge is 30.48 m in length. The bridge cross section consists of five identical steel girders spaced at a distance of 2.13 m. The bridge cross section is illustrated in Fig. 1. Some basic sizes and material properties of the bridge are listed in Table 1.

The finite element (FE) method was used to analyze the bridge responses under repeated vehicle loading under different corrosion conditions. A three-dimensional (3D) finite element bridge model, as illustrated in Fig. 2, was created for the bridge. Two end diaphragms and three intermediate diaphragms were arranged for more even distribution of loads among the girders [15]. The steel girders, the concrete bridge deck, and the guardrail were all modeled by solid elements. The diaphragms were modeled by shell elements.

2.2. Truck models

In this study, the design fatigue truck HS 20–44 specified in the AASHTO fatigue guide specifications [17] was used in calculating the cumulative fatigue damage of the bridge in the numerical study. This three-axle truck, as shown in Fig. 3, has the static axle weights (W_A) of 35.84 kN, 142.08 kN, and 142.08 kN for the first, second, and third axles, respectively. It is noteworthy that the gross weight of the AASHTO design fatigue truck was developed from the actual traffic spectrum collected from 30 weigh-in-motion (WIM) sites in the United States which covered more than 27,000 trucks [18]. Its configuration was determined based on the axle weight ratios and axle spacings of the four- and five-axle trucks on the road which contribute largely to the fatigue damage of bridges [19]. Moreover, it has been demonstrated that the cumulative fatigue damage caused by the AASHTO fatigue truck during a certain time period was close to that caused by the real

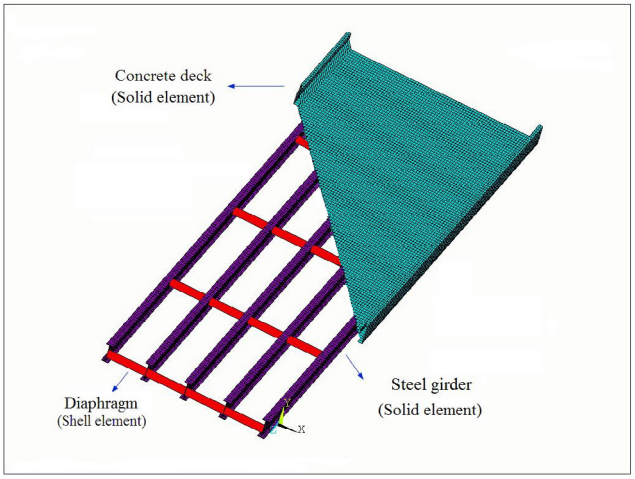

Fig. 2. 3D FE bridge model.

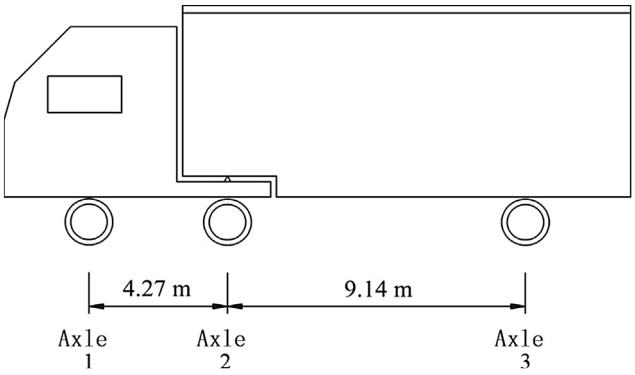

Fig. 3. Sketch of the design fatigue truck model.

truck traffic flow [15]. Since trucks are more likely to be axle-load overloading rather than the gross-weight overloading according to a Tennessee study [20], axle-based overweight was considered in this study. Four overloading conditions were considered in the present study, in which the axle weights were set to 1.25, 1.50, 1.75, and 2.00 times the axle weights of the design fatigue truck, respectively. They are good representatives of the weights of overweight trucks according to the truck weight survey conducted by Schilling and Klippstein [21]. It is noted that in order to investigate the relationship between the overweight ratio and the induced damage on the bridge, the weight difference between the overweight trucks was set to be the same on purpose. In addition, the same configuration as the design fatigue truck was adopted for the overweight trucks in order to avoid making the problem too complicated.

It should be mentioned that the probability of multiple truck presence on a bridge is relatively small [22,23]. Therefore, only the case with a single truck traveling in the slow lane, as suggested by the AASHTO LRFD code [5], was considered in the fatigue analysis in the present study.

2.3. Corrosion model

Deterioration affects various structural components of bridges to

Table 1
Basic properties of the bridge considered.

Roadway width	Concrete deck thickness	Girder height	Cross-sectional area	Moment of inertia	Young's modulus	Poisson's ratio
9.75 (m)	0.20 (m)	1.61 (m)	0.02 (m^2)	0.0011 (m^4)	210 (GPa)	0.25

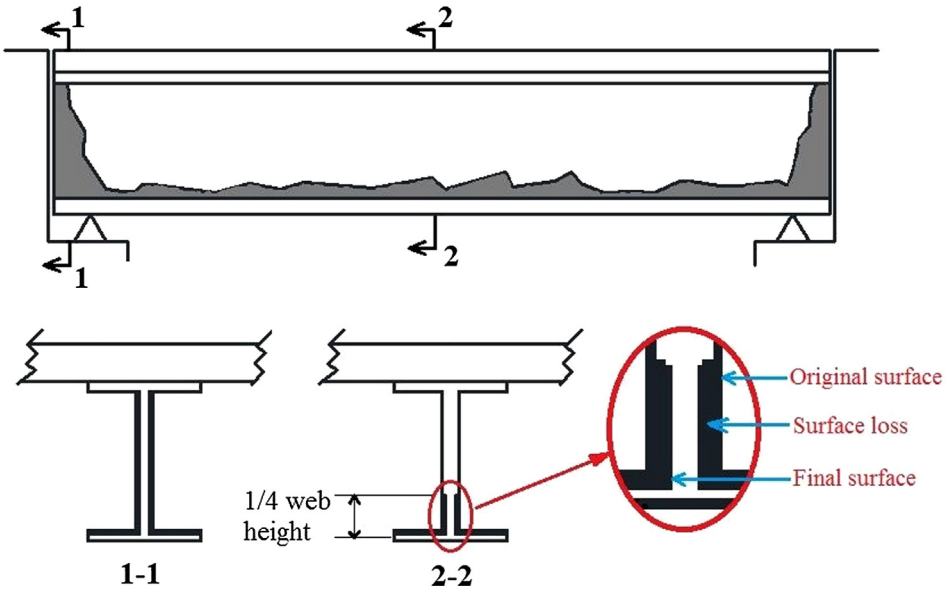

Fig. 4. Typical locations of corrosion on the steel girder.

different degrees [24]. The fatigue and corrosion of girders could lead to a considerable reduction of the load-carrying capacity of bridges. The deterioration of bridge deck, on the other hand, could affect the serviceability of the bridge but not necessarily threaten the bridge safety. Therefore, only the corrosion of the girders was considered in this study.

The most common effect due to corrosion is the loss of material [25]. In this study, uniform reduction of the cross section of the girder was assumed when considering the corrosion. In addition, field surveys show that corrosion usually occurs at two places, namely, the entire web near the supports due to deck joint leakage [2] and the top surface of the bottom flange due to the accumulation of dust on undrained surfaces or the accumulation of road spray and traffic deicer spray [24], as illustrated in Fig. 4. It should be noted that at the bridge mid-span, the corrosion of web usually reaches 1/4 of the web height [25].

Generally, corrosion does not take place immediately after bridge erection due to the protection of the paint and the protective covers. However, as the protection deteriorates, corrosion penetration grows exponentially [26], which can be illustrated using the equation below:

$$r = r_A \times t^{r_B} \tag{1}$$

where r denotes the average corrosion depth (in μm) after t years of exposure; r_A is the corrosion loss after one year of exposure; and r_B is a regression coefficient determined from experimental data. Based on the level of corrosion condition, marine, urban, and rural environments are usually classified into environments with high, medium and low levels of corrosion, respectively, and the corresponding average values of r_A and r_B for carbon steel in these environments are listed in Table 2 [6].

It should be noted that for the selected corrosion model shown in Eq. (1), corrosion was assumed to start immediately since bridge erection which is contradictory to the fact. Therefore, there is a need to improve the corrosion model. According to Park and Nowak [27], the corrosion depth calculated from Eq. (1) is revised as shown in Fig. 5, in which corrosion starts from the 5th, 10th, and 15th year under the marine, urban and rural environments, respectively. In addition, exterior and interior girders were assumed to have the same corrosion rate, as did by other researchers [25].

Table 2
Average values for corrosion parameters r_A and r_B.

Environment	Carbon steel	
	r_A	r_B
Rural	34.0	0.65
Urban	80.2	0.59
Marine	70.6	0.79

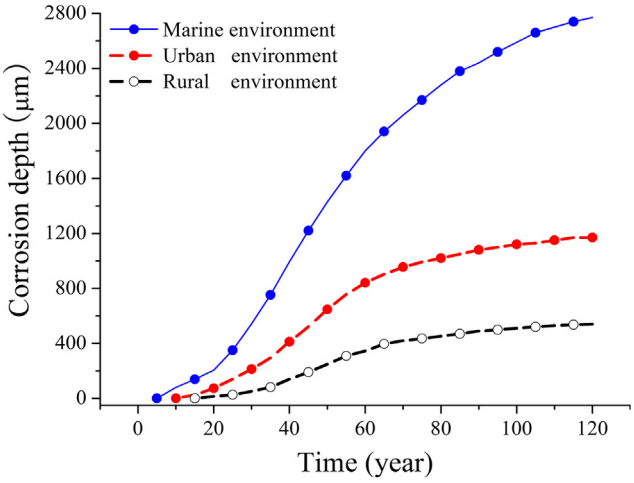

Fig. 5. Corrosion penetration of the steel girders.

3. Cumulative corrosion fatigue damage of bridges

Under repeated truck overloading, bridge components deteriorate due to the cumulative fatigue damage, and cracking in the steel girders may be initiated as a result. Around the cracks, the accumulated chloride can promote the initiation and development of corrosion on the steel girders. As a result, the effective cross section of the steel girder will decrease, resulting in an increase in stress. The increasing stress could in turn accelerate the development of corrosion and cause more severe fatigue damage on the bridge. Finally, the coupled corrosion-overloading effect will speed up the deterioration of the bridge and shorten its service life. In this study, for the purpose of computational convenience, the corrosion-overloading coupling process was realized by adopting reduced cross sections of the steel girder due to corrosion when calculating the bridge responses under the action of truck overloading.

In this study, the Miner's rule [28], as suggested by the AASHTO LRFD code for calculating the fatigue damage of bridges, was adopted to calculate the effective bending and shear stress ranges. It is noted that Miner's rule has been widely applied in bridge fatigue design [29]. Based on the stress obtained from the finite element analysis, the cumulative fatigue damage (Cumulative FD) can then be calculated as follows:

$$Cumulative\ FD(t) \sum_i \frac{n_i}{N_i} \tag{2}$$

where n_i denotes the number of stress cycles experienced that are within the ith stress-range S_i; N_i denotes the number of stress cycles to failure for the predefined stress-range S_i. If no corrosion is considered, the relationship between N_i and S_i can be defined as [5]:

$$N_i = \frac{A}{S_i^m} \tag{3}$$

where A is a constant given in the design specifications based on the category of the detail under consideration; and m is the slope constant of the S-N curve, which was determined based on the fatigue details investigated, such as the welds between the bottom flange and the web of the steel girders in this study. In addition, the fatigue constants A are taken as 3.93×10^{12} MPa and 6.55×10^{15} MPa for the details assessed based on the bending stress and shear stress, respectively [30]. The slope constants m are taken as 3 and 5 for the details assessed for bending stress and shear stress, respectively [30].

Based on Schilling's study [31], the cumulative fatigue damage induced by truck passage can be calcualted using the maximum stress range (MSR) and the equivalent number of stress cycles (ENSC) can be determined as follows:

$$ENSC = num + \left(\frac{S_{r1}}{S_{rp}}\right)^m + \left(\frac{S_{r2}}{S_{rp}}\right)^m + \cdots + \left(\frac{S_{ri}}{S_{rp}}\right)^m \tag{4}$$

where *num* is the number of MSR due to a single truck passage; S_{ri} are the higher-order stress ranges; and S_{rp} is the primary stress range, and can be calculated as the algebraic difference between the maximum stress and the minimum stress.

In calculating the ENSC in the present study, the effecitve bending stress range was set to 3.45 MPa to 33% of the CAFL according to [32,33] while the cut-off limit for the shear stess was set to 45.7% of the detail constant (i.e., A in Eq. (3)) according to [34]. Moreover, the number of stress cycles was determined based on the rainflow counting algorithm [35]. In addition, to account for the dynamic effect of the truck loading, an impact factor of 0.15 was adopted, as suggested by the AASHTO LRFD code [5]. Finally, based on the Miner's cumulative damage model, the cumulative fatigue damage due to the truck loading during a predefined time interval ΔT can be calculated using the following equation:

$$Cumulative \quad FD = Num \cdot \frac{ENSC \cdot MSR^m}{A} \tag{5}$$

where *Num* is the number of truck passage during a given time period ΔT.

It is noted that for corrosion conditions, the relationship in Eq. (3) should be updated to Eq. (6) and the induced cumulative fatigue damage in Eq. (5) is therefore calculated with parameters adjusted considering the corrosion conditions correspondingly.

$$N_i = \frac{A'}{S_{corr\_i}^m} \tag{6}$$

where $A' = A/K_f$, and K_f is the fatigue reduction factor which equals to $1.2 + 5.77r$ [36], where r is the corrosion depth which can be obtained from Fig. 5; S_{corr_i} is the stress range adjusted to account for the section reduction of the steel girder due to corrosion in this study; and m is generally taken as 3.26 and 7 for the bending stress and shear stress under corrosive environment [36,37].

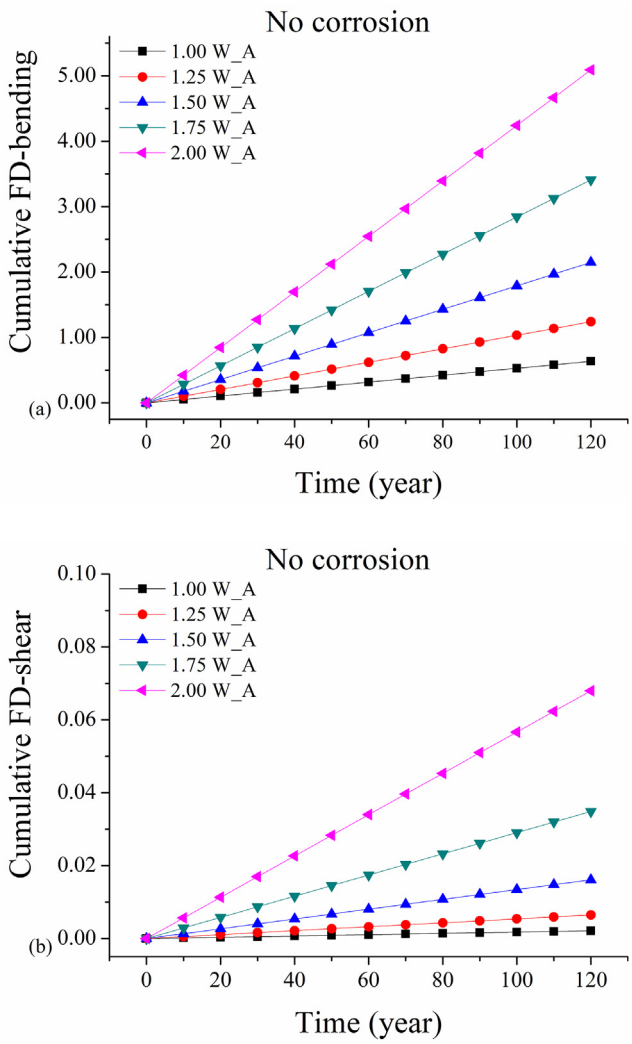

Fig. 6. Cumulative FD caused by trucks with different axle weights.

4. Numerical results

For small-to-medium-span bridges, bending moment is generally believed to be more critical than shear force to satisfy the bridge section requirement [25,38,39]. Nevertheless, the shear capacity could become more critical than bending moment after a certain period of time due to corrosion [24]. Therefore, both the bending stress at the girder midspan and the shear stress near the supports were considered in the present study. Three corrosion conditions, i.e., low, medium, and high corrosion conditions were considered. Five truck weights, namely, 1.00 W_A, 1.25 W_A, 1.50 W_A, 1.75 W_A, and 2.00 W_A (W_A denotes the axle weights of the design fatigue truck) were adopted to investigate the coupled corrosion-overloading effect on the bridge.

4.1. Cumulative FD considering the coupled corrosion-overloading effect

Fig. 6 shows the cumulative fatigue damage based on the bending stress and shear stress of the steel girder under the loading of trucks with 1.00 W_A, 1.25 W_A, 1.50 W_A, 1.75 W_A, and 2.00 W_A without considering corrosion. It can be easily seen from Fig. 6 that without considering corrosion, the Cumulative FD of the bridge, due to either the bending stress or the shear stress, increases linearly with time. This is due to the linear fatigue damage model adopted in this study. In

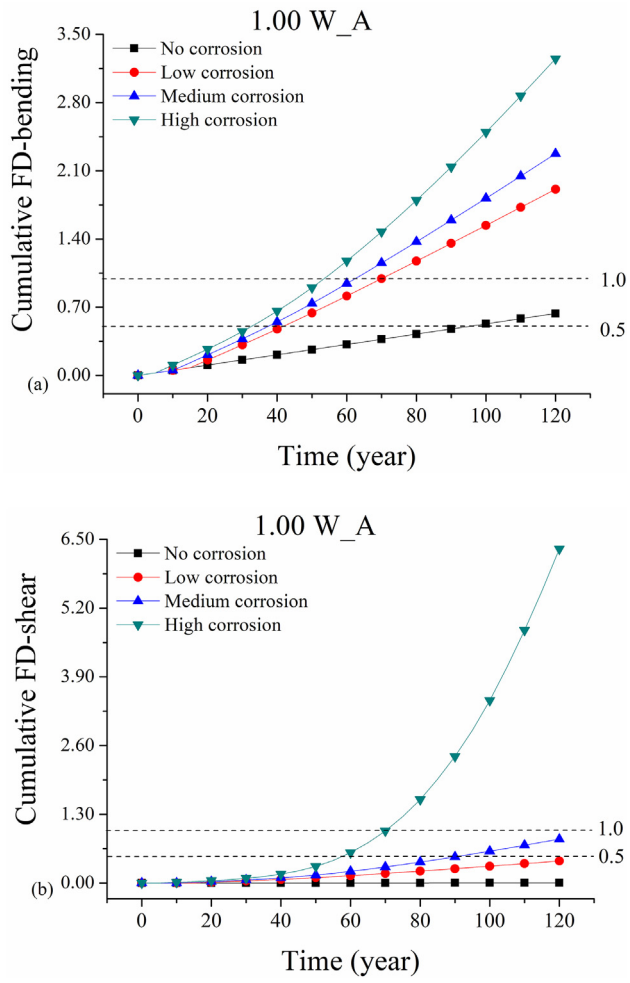

Fig. 7. Cumulative fatigue damage of the steel girder under different corrosion conditions.

addition, the Cumulative FD increases more rapidly than the increase of the vehicle axle weight. This is because the fatigue damage is proportional to the third power of the stress range (and therefore the third power of the axle weight), as demonstrated by Eq. (6). It should be mentioned that a Cumulative FD of greater than 1.0 is meaningless in practice and the only reason why the Cumulative FD over 1.0 was plotted in the following figures is to show the variation trend more clearly.

Fig. 7 displays the calculated cumulative fatigue damage based on the bending stress and shear stress under different corrosion conditions and the action of the design fatigue truck (1.00 W_A). As can be seen from Fig. 7 that the fatigue damage under corrosion is apparently larger than that without considering corrosion and the difference becomes larger as the corrosion condition becomes more severe. It is also interesting to note that fatigue damage accumulates nonlinearly with time under corrosive environments, which is different from the cases without corrosion. Moreover, the nonlinear variation trend tends to be more distinct as the degree of corrosion varies from low to high.

It can be predicted from Fig. 6(a) that the Cumulative FD of the bridge without corrosion reached 1.0 after 190 years. In contrast, it takes only 71 years, 63 years and 54 years for the Cumulative FD to reach 1.0 under low, medium, and high corrosion conditions, respectively, as shown in Fig. 7(a). In other words, the fatigue life is reduced by 62.63%, 66.84%, and 71.58%, respectively under these three different corrosion conditions. This is consistent with the findings by Zhang and Yuan [2], in which more than 60% reduction of fatigue life can be predicted under different corrosion conditions. In this regard,

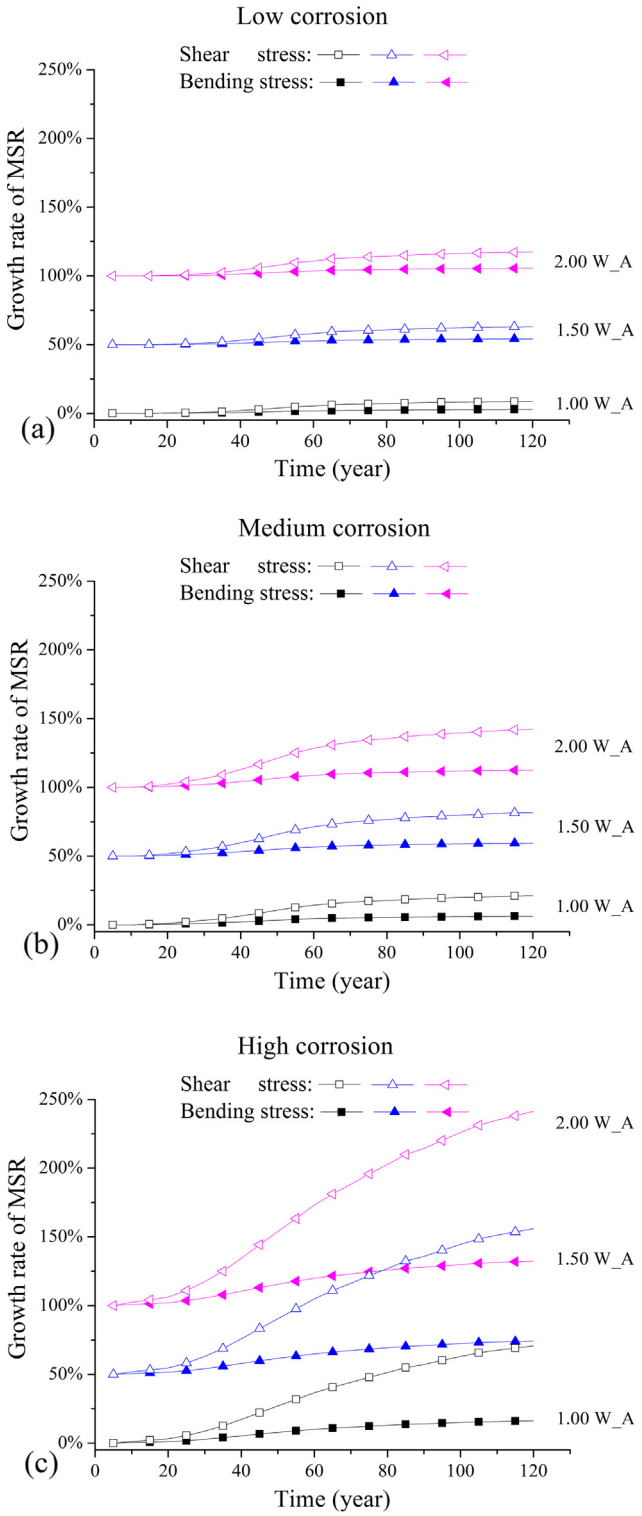

Fig. 8. Coupled corrosion-overloading effect on the MSR based on the bending stress and shear stress.

the corrosion effect should not be neglected in the fatigue design of bridges. Furthermore, as can be seen from Fig. 7(a) that the fatigue damage will reach 0.5 after 37 years under urban environment which is a normal corrosion condition. This prediction is generally consistent with the finding of INDOT that the bridge would deteriorate to poor condition (rating of 4) after around 40 years of service under normal corrosion condition [40,41]. A poor condition of the bridge structure in general corresponds to a fatigue damage of 0.5 [41].

4.2. Coupled corrosion-overloading effect on the MSR and ENSC

From Eq. (6) it can be seen that the MSR and ENSC are two primary parameters that determine the Cumulative FD. To investigate the coupled corrosion-overloading effect, the growth rates of MSR based on the bending stress and shear stress under different corrosion conditions are plotted in Fig. 8. It should be mentioned that in order to show the variation clearly, only the growth rates of MSR under the loading of trucks with 1.00 W_A, 1.50 W_A, and 2.00 W_A are plotted in Fig. 8.

Based on Fig. 8, it is obvious that the growth rate of the MSR of shear stress (MSR_shear) increases more rapidly than that of bending stress (MSR_bending) as the corrosion condition becomes more severe. Moreover, the growth rate of MSR_shear is always larger than that of MSR_bending, and their difference becomes more apparent as the corrosion depth increases. In fact, shear force is mainly carried by the web of the bridge girder which is vulnerable to corrosion, especially near the supports where corrosion can affect the whole web height. As a result, the shear stress is more sensitive to the corrosion condition than the bending stress, as shown in Fig. 8. Thus, special attention should be paid to shear when conducting the corrosion fatigue design.

In addition, the coupled corrosion-overloading effect on the ENSC was also investigated. Table 3 shows the growth rates of the ENSC of bending stress under high corrosion and noncorrosive conditions. For the purpose of illustration, only the results under the loading of trucks with 1.00 W_A, 1.50 W_A, and 2.00 W_A are listed in Table 3. It can be found that the variation of ENSC is much less than 1% and is therefore negligible even under high corrosion and severe overloading conditions. What's more, the variation of the ENSC does not follow a certain trend, suggesting that ENSC may not be a good indicator of the cumulative fatigue damage.

5. Corrosion fatigue design method considering the coupled corrosion-overloading effect

Since the MSR is predominant for the fatigue damage as discussed earlier, the corrosion fatigue design method proposed in this study is based on the MSR. In this study, the stress considering the coupled corrosion-overloading effect was considered as a combination of the individual stress range caused by each of the three parts, i.e., pure overloading, pure corrosion, and the corrosion-overloading interaction. For the purpose of illustration, a composite steel girder bridge was used in the present study as an example. The fatigue design method considering the coupled corrosion-overloading effect was conducted as follows:

Table 3
Variation of the ENSC under different corrosive environments.

Time (year)	ENSC under noncorrosive condition			ENSC under high corrosion condition		
	1.00 W_A	1.50 W_A	2.00 W_A	1.00 W_A	1.50 W_A	2.00 W_A
5	0.00%	0.09%	0.09%	0.00%	0.09%	0.09%
10	0.00%	0.09%	0.09%	−0.05%	0.00%	0.00%
15	0.00%	0.09%	0.09%	−0.05%	0.00%	0.00%
20	0.00%	0.09%	0.09%	−0.05%	0.00%	0.00%
25	0.00%	0.09%	0.09%	−0.05%	0.00%	0.00%
30	0.00%	0.09%	0.09%	−0.05%	0.00%	0.00%
35	0.00%	0.09%	0.09%	−0.05%	0.00%	0.00%
40	0.00%	0.09%	0.09%	−0.04%	0.00%	0.00%
45	0.00%	0.09%	0.09%	−0.04%	0.01%	0.01%
50	0.00%	0.09%	0.09%	−0.04%	0.01%	0.01%
55	0.00%	0.09%	0.09%	−0.04%	0.01%	0.01%
60	0.00%	0.09%	0.09%	−0.03%	0.01%	0.01%
65	0.00%	0.09%	0.09%	−0.03%	0.02%	0.02%
70	0.00%	0.09%	0.09%	−0.03%	0.02%	0.02%
75	0.00%	0.09%	0.09%	−0.02%	0.02%	0.02%

(1) Calculate the growth rate of MSR due to pure overloading (Δ_{OL})

The vehicle-induced stress is closely related to the vehicle axle weight and axle spacing, etc. In this study, the growth rate of the stress range can be calculated according to Eq. (7) to account for the influence of overloading. Moreover, since the overweight trucks adopted in this study has a same configuration with the design fatigue truck, the stress range caused by overweight trucks can be easily estimated based on the axle weight ratio. Specifically, the stress range increment under the loading of trucks with 1.25 W_A, 1.50 W_A, 1.75 W_A, and 2.00 W_A is in accordance with their axle weight increment, namely, 25%, 50%, 75%, and 100%, respectively, as can be obtained from Fig. 6.

$$\Delta_{OL} = \frac{MSR_{OL} - MSR_0}{MSR_0} \tag{7}$$

where MSR_{OL} and MSR_0 are the maximum stress ranges caused by the overweight truck and the design fatigue truck, respectively, under non-corrosive environment.

(2) Calculate the growth rate of MSR due to corrosion (Δ_{Cor})

In this study, it was assumed that the effect of pure corrosion on the growth rate of MSR does not change with the truck load on the bridge. In other words, the effect of pure corrosion can be calculated based on the difference between the stress ranges caused by the design fatigue truck under corrosive and non-corrosive environment, as shown in Eq. (8).

$$\Delta_{Cor} = \frac{MSR_{Cor} - MSR_0}{MSR_0} \tag{8}$$

where MSR_{Cor} is the maximum stress range caused by the design fatigue truck under corrosive environment.

In addition, Fig. 9 displays the Δ_{Cor} based on bending stress ($\Delta_{Cor\_bending}$) and the Δ_{Cor} based on shear stress (Δ_{Cor_shear}), respectively, under the loading of the design fatigue truck. It can be seen from Fig. 9 that the growth rates of the MSR under corrosive environment increase with time in a similar fashion with the development of corrosion depth shown in Fig. 5. However, the growth rate of MSR_shear in Fig. 9(b) is much higher than that of MSR_bending in Fig. 9(a), which is probably due to the fact that the shear stress is more sensitive to the corrosion condition, as discussed previously.

(3) Calculate the growth rate of MSR due to the corrosion-overloading interaction (Δ_{Coup})

In this study, based on the MSR_{OL} and MSR_{Cor} obtained in the previous two steps and the stress range considering the coupled corrosion-overloading effect (MSR_C), as shown in Fig. 8, the stress range due to the corrosion-overloading interaction (MSR_{Coup}) can be calculated as follows:

$$MSR_{Coup} = MSR_C - MSR_{OL} - MSR_{Cor} \tag{9}$$

Then, the growth rate of MSR due to the corrosion-overloading interaction (Δ_{Coup}) can be obtained according to Eq. (10) below. The results are shown in Fig. 10.

$$\Delta_{Coup} = \frac{MSR_{Coup} - MSR_0}{MSR_0} \tag{10}$$

It can be seen from Fig. 10(a) that the Δ_{Coup} based on bending stress ($\Delta_{Coup\_bending}$) increases with the increase of the vehicle axle weight and the maximum growth rate reaches 8.41%. In contrast, the Δ_{Coup} based on shear stress (Δ_{Coup_shear}) increases more rapidly with time and its maximum value reaches 33.48% under the loading of the truck with 2.0 W_A.

It is worthwhile to point out that similar to Δ_{Cor}, the variation of Δ_{Coup} in Fig. 10 also shows a similar trend with the development of

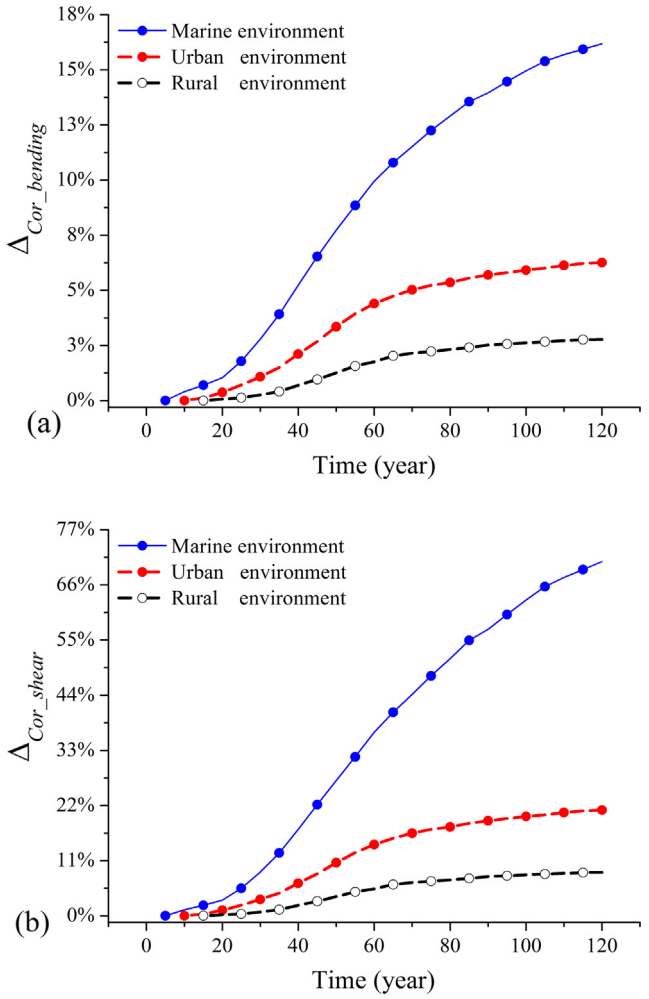

Fig. 9. Growth rates of the MSR under different corrosive environments.

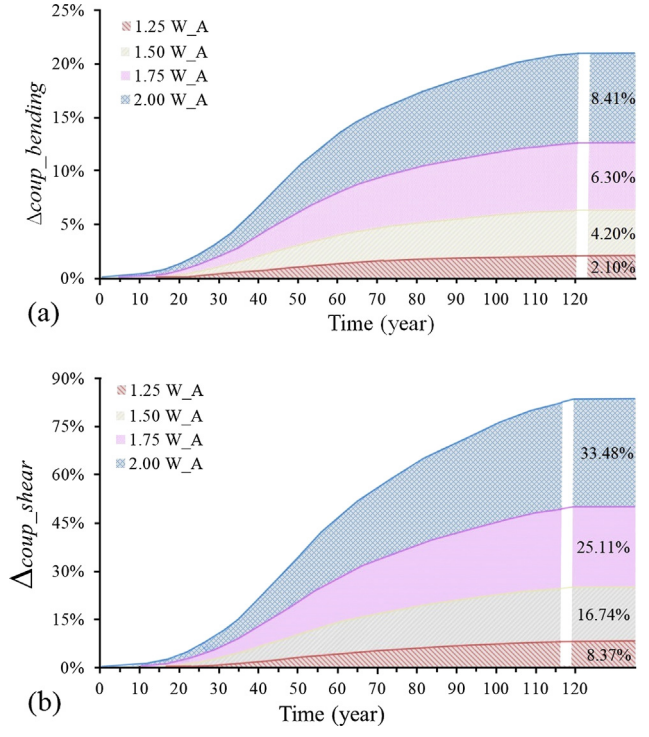

Fig. 10. Growth rates of the MSR due to the corrosion-overloading interaction.

Table 4
Parameters for $\Delta_{Coup\_bending}$.

Parameter	High corrosion	Medium corrosion	Low corrosion	Corrosion average
Y	−0.112	−0.131	−0.205	−0.078
W	0.112	0.131	0.205	0.078
C	0.009	0.010	0.016	0.006
R^2	100.000%	99.998%	99.993%	99.998%

corrosion depth as shown in Fig. 5. More importantly, it is observed in Fig. 10 that Δ_{Coup} for trucks with 2.00 W_A, 1.75 W_A, and 1.50 W_A is 4, 3, and 2 times that for the truck with 1.25 W_A, respectively. Therefore, only the relationship between the corrosion depth (r) and the Δ_{Coup} for the truck with 1.25 W_A was investigated in the following. Based on the regression analysis on the simulation data, the following expression can be used to describe this relationship:

$$\Delta_{Coup} = Y + W \times e^{r/C} \tag{11}$$

where Y, W, and C are the parameters obtained based on curve fitting, and the parameter values for $\Delta_{Coup\_bending}$ and Δ_{Coup_shear} are listed in Tables 4 and 5, respectively.

The goodness of fit for the model described by Eq. (11) was then checked and the results are also summarized in Tables 4 and 5. From Tables 4 and 5, it is obvious that R^2, the goodness of fit, is very close or equal to 100% under all the cases considered. Therefore, these results suggest that the relationship between Δ_{Coup} and the corrosion depth (r) can be well described by the exponential function in Eq. (11). This finding is consistent with the test results in [1].

(4) Fatigue life of bridges considering the coupled corrosion-overloading effect

It should be noted that although Δ_{Cor} and Δ_{Coup} are obtained based on the bridge selected in this study, Δ_{Cor} can be used for vehicles with different axle weights directly while Δ_{Coup} for trucks with different axle weights can be calculated easily using interpolation method. In addition, Δ_{OL} can be easily estimated based on the axle weight ratio and axle spacing, etc. As a result, the stress range considering the coupled corrosion-overloading effect can be calculated easily according to Eq. (12).

$$MSR_c = MSR_0(1 + \Delta_{OL} + \Delta_{Cor} + \Delta_{Coup}) \tag{12}$$

Then, the cumulative fatigue damage of the bridge under different corrosion and overloading conditions can be calculated according to Eq. (13). It should be mentioned that in order to reduce the computational effort, the *ENSC* employed in Eq. (13) does not consider the influence of corrosion and overloading, because the variation of *ENSC* under the corrosion and overloading conditions is negligible, as mentioned previously.

$$Cummlative\ FD_c = Num \cdot \frac{ENSC \cdot MSR_c^m}{A} \tag{13}$$

Finally, the fatigue life of the bridge under different corrosion and overloading conditions were calculated and the results are presented in Table 6. In addition, the life reduction due to the corrosion and overloading is also listed in Table 6 for the purpose of comparison. It should

Table 5
Parameters for Δ_{Coup_shear}

Parameter	High corrosion	Medium corrosion	Low corrosion	Corrosion average
Y	−0.085	−0.109	−0.121	−0.056
W	0.085	0.109	0.121	0.057
C	0.002	0.003	0.003	0.002
R^2	99.996%	100.000%	99.999%	99.986%

Table 6
Fatigue life of bridges under different corrosion and overloading conditions

Overloading only			Corrosion only			Coupled corrosion-overloading	
Overloading condition	Fatigue life (year)	Life reduction	Corrosion condition	Fatigue life (year)	Life reduction	Fatigue life (year)	Life reduction
Design fatigue truck (0% overloading)	190	–	Low	71	62.63%	–	–
			Medium	63	66.84%	–	–
			High	54	71.58%	–	–
25% overloading	97	48.95%	Low	71	62.63%	41	78.42%
			Medium	63	66.84%	36	81.05%
			High	54	71.58%	31	83.68%
50% overloading	56	70.53%	Low	71	62.63%	28	85.26%
			Medium	63	66.84%	24	87.37%
			High	54	71.58%	20	89.47%
75% overloading	35	81.58%	Low	71	62.63%	21	88.95%
			Medium	63	66.84%	17	91.05%
			High	54	71.58%	14	92.63%
100% overloading	24	87.37%	Low	71	62.63%	17	91.05%
			Medium	63	66.84%	14	92.63%
			High	54	71.58%	10	94.74%

be noted that the fatigue life under the loading of design fatigue truck (HS 20-44 truck) without considering corrosion, namely, 190 years, can be regarded as the design fatigue life for the bridge investigated according to AASHTO LRFD codes [5]. As can be seen from Table 6 that under the coupled effect of low corrosion and 25% overloading, the fatigue life reduction can be nearly 15% and 30% larger than when the corrosion and the overloading are applied separately, even though the growth rate of stress range due to the corrosion-overloading interaction. This indicates the importance of considering the corrosion-overloading interaction when evaluating the fatigue life of bridges. In addition, it can be seen from Table 6 that the reduction of fatigue life under the coupled corrosion-overloading effect is much smaller than the algebraic sum of the individual effect of the corrosion and overloading but higher than the effect under either one acting separately. This indicates that the coupled corrosion-overloading effect on the reduction of fatigue life is not a simple additive process and simply adding the individual effects due to corrosion and overloading up could lead to considerable overestimation of the corrosion fatigue damage. This finding confirms the necessity of developing a simple corrosion fatigue method for bridges.

6. Summary and conclusions

In the present study, a steel I-girder bridge was adopted as an example to investigate the coupled corrosion-overloading effect on the fatigue life of bridges. It was found that the coupled corrosion-overloading effect could result in considerable reduction of fatigue life of bridges while simply adding the individual effects due to corrosion and overloading up could lead to considerable overestimation of the corrosion fatigue damage. In addition, a simple corrosion fatigue design method for bridges was proposed by considering the coupled corrosion-overloading effect. Based on the results from this study, some concluding remarks can be drawn as follows:

(1) The fatigue life of the bridge investigated can be reduced by 62.63%, 66.84%, and 71.58% under the rural, urban and marine environment, respectively, as compared to the design fatigue life calculated according to the AASHTO LFRD codes. This indicates that a corrosive environment can severely reduce the bridge fatigue life and should not be neglected in the bridge fatigue design.
(2) Under corrosion and overloading conditions, the accumulation of bridge fatigue damage exhibits nonlinear characteristics as compared to the linear feature under pure overloading condition.
(3) The cumulative fatigue damage due to shear stress increases dramatically as the corrosion condition turns worse while it is not the case for fatigue damage due to bending stress. This implies that the shear stress is more sensitive to corrosive environment and should be paid special attention in the corrosion fatigue design.

Besides the proposed corrosion fatigue design method, the results obtained in this study could provide useful information for the damage estimation of existing bridges under different corrosion and/or overloading conditions.

Acknowledgement

The authors gratefully acknowledge the financial support provided by the National Natural Science Foundation of China (Grant No. 51478176 and 51778222), the Key Research Project of Hunan Province (Grant 2017SK2224), and the China Scholarship Council (No. 201706130087).

References

[1] Yang S, Yang H, Liu G, Huang Y, Wang L. Approach for fatigue damage assessment of welded structure considering coupling effect between stress and corrosion. Int J Fatigue 2016;88:88–95.
[2] Zhang W, Yuan H. Corrosion fatigue effects on life estimation of deteriorated bridges under vehicle impacts. Eng Struct 2014;71:128–36.
[3] Yang DH, Yi TH, Li HN. Coupled fatigue-corrosion failure analysis and performance assessment of RC bridge deck slabs. J Bridge Eng 2017;22(10):04017077.
[4] Zmetra KM, McMullen KF, Zaghi AE, Wille K. Experimental study of UHPC repair for corrosion-damaged steel girder ends. J Bridge Eng 2017;22(8):04017037.
[5] American Association of State Highway and Transportation Officials (AASHTO). LRFD bridge design specifications. Washington, D.C.; 2017.
[6] Albrecht P, Naeemi AH. Performance of weathering steel in bridges. NCHRP Report 272; 1984.
[7] Berwick B. Calibrating the steel-members fatigue limit states of the AASHTO LRFD bridge design specifications. University of Delaware; 2012.
[8] Keating PB, Fisher JW. Review of fatigue tests and design criteria on welded details Fritz Engineering Laboratory Report 488–1(85). Bethlehem, Penn: Lehigh University; 1986.
[9] Zhang W, Wu M, Zhu J. Evaluation of vehicular dynamic effects for the life cycle fatigue design of short-span bridges. Steel Constr 2017;10(1):37–46.
[10] Stephens RI, Ratemi A, Stephens RR, Fuchs HO. Metal fatigue in engineering. 2nd ed. New York, NY: John Wiley & Sons; 2000.
[11] Kayser JR, Nowak AS. Evaluation of corroded steel bridges. In: Tall L, editor. Bridges and transmission line structures. New York, NY: ASCE; 1987.
[12] Cha H, Liu B, Prakash A, Varma AH. Effect of local damage caused by overweight trucks on the durability of steel bridges. J Perform Constr 2014;30(1):04014183.
[13] Biondini F, Frangopol DM. Life-cycle performance of deteriorating structural systems under uncertainty. J Struct Eng 2016;142(9):F4016001.
[14] American Association of State Highway and Transportation Officials (AASHTO). Standard specifications for highway bridges. Washington, D.C.; 2012.
[15] Wang TL, Liu C, Huang D, Shahawy M. Truck loading and fatigue damage analysis for girder bridges based on weigh-in-motion data. J Bridge Eng 2005;10(1):12–20.
[16] Wang W, Deng L, Shao X. Number of stress cycles for fatigue design of simply-supported steel I-girder bridges considering the dynamic effect of vehicle loading. Eng Struct 2016;110:70–8.
[17] American Association of State Highway and Transportation Officials (AASHTO). Guide specifications for fatigue evaluation of existing steel bridges. Washington, D.C.; 1990.

[18] Snyder RE, Likins GE, Moses F. Loading spectrum experienced by bridge structures in the United States Report No. FHWA/RD-85/012. Warrensville, Ohio: Bridge Weighing Systems Inc.; 1985.
[19] Schilling CG, Klippstein KH. New method for fatigue design of bridges. J Struct Div 1978;104(3):425–38.
[20] Siekmann A, Capps G, Hudson MBL. Preliminary assessment of overweight mainline vehicles. Rep. prepared for Oak Ridge National Laboratory, Oak Ridge, TN; 2011.
[21] Schilling CG, Klippstein KH. Fatigue of steel beams by simulated bridge traffic. J Struct Div 1977;105(1):260–1.
[22] Zhang W, Cai CS. Fatigue reliability assessment for existing bridges considering vehicle speed and road surface conditions. J Bridge Eng 2011;17(3):443–53.
[23] Nowak AS, Nassif H, DeFrain L. Effect of truck loads on bridges. J Transp Eng 1993;119(6):853–67.
[24] Kayser JR, Nowak AS. Capacity loss due to corrosion in steel-girder bridges. J Struct Eng 1989;115(6):1525–37.
[25] Czarnecki AA, Nowak AS. Time-variant reliability profiles for steel girder bridges. Struct Saf 2008;30(1):49–64.
[26] Komp ME. Atmospheric corrosion ratings of weathering steels-calculation and significance. Mater Perform 1987;26(7):42–4.
[27] Park CH, Nowak AS. Lifetime reliability model for steel girder bridges. In: Das PC, editor. Safety of bridges. London: Thomas Telford Publishing; 1997.
[28] Miner MA. Cumulative damage in fatigue. J Appl Mech 1945;12(3):159–64.
[29] Fatemi A, Yang L. Cumulative fatigue damage and life prediction theories: a survey of the state of the art for homogeneous materials. Int J Fatigue 1998;20(1):9–34.
[30] Hobbacher A. Recommendations for fatigue design of welded joints and components. New York: Welding Research Council; 2009.
[31] Schilling CG. Stress cycles for fatigue design of steel bridges. J Struct Eng 1984;110(6):1222–34.
[32] Kwon K, Frangopol DM, Soliman M. Probabilistic fatigue life estimation of steel bridges by using a bilinear S-N approach. J Bridge Eng 2012;17(1):58–70.
[33] Connor R, Hodgson I, Mahmoud H, Bowman C. Field testing and fatigue evaluation of the I-79 Neville Island Bridge over the Ohio River. Bethlehem (PA): Lehigh University's Center for Advanced Technology for Large Structural Systems (ATLSS); 2005.
[34] Wendimu A. Fatigue life estimation of existing steel structures under time-dependent structural degradation. Norway: University of Stavanger; 2014.
[35] Downing SD, Socie DF. Simple rainflow counting algorithms. Int J Fatigue 1982;4(1):31–40.
[36] Hahin C. Effects of corrosion and fatigue on the load carrying capacity of structural and reinforcing steel. Illinois Dept Transport Bureau Mater Phys Res 1994.
[37] Gassner E, Schütz W. Assessment of the allowable design stresses and the corresponding fatigue life. Proc 4th symposium of the corresponding fatigue: fatigue design procedures. Munich, Germany. 1965.
[38] Brühwiler E, Herwig A. Consideration of dynamic traffic action effects on existing bridges at ultimate limit state. In: Koh Fragopol, editor. Bridge maintenance, safety, management, health monitoring and informatics. London: Taylor & Francis Group; 2008.
[39] González A, Cantero D, OBrien EJ. Dynamic increment for shear force due to heavy vehicles crossing a highway bridge. Comput Struct 2011;89(23–24):2261–72.
[40] Sinha K, Labi S, McCullouch B, Bhargava A, Bai Q. Updating and enhancing the Indiana Bridge Management System (IBMS). FHWA/IN/JTRP-2008/30, joint transportation research program of Indiana Dept. of Transportation and Purdue Univ., West Lafayette, IN; 2009.
[41] Indiana Department of Transportation. Bridge inspection manual. Indianapolis, IN; 2010. 〈http://www.in.gov/dot/div/contracts/standards/bridge/ inspector_manual/〉 [Sep. 17, 2014].